Accumulation of aberrant ubiquitin induces aggregate formation and cell death in polyglutamine diseases

Pril, R.de; Fischer, D.F.; Maat-Schieman, M.L.C.; Hobo, B.; Vos, R.A.I.de; Brunt, E.R.; Hol, E.M.; Roos, R.A.C.; Leeuwen, F.W.van

Published in:
Human Molecular Genetics

DOI:
10.1093/hmg/ddh188

Publication date:
2004

Human Molecular Genetics, 2004, Vol. 13, No. 16 ***1803–1813***
doi:10.1093/hmg/ddh188
Advance Access published on June 15, 2004

Accumulation of aberrant ubiquitin induces aggregate formation and cell death in polyglutamine diseases

Remko de Pril[1], David F. Fischer[1], Marion L.C. Maat-Schieman[2], Barbara Hobo[1], Rob A.I. de Vos[3], Ewout R. Brunt[4], Elly M. Hol[1], Raymund A.C. Roos[2] and Fred W. van Leeuwen[1,*]

[1]Research Team Molecular Misreading, Netherlands Institute for Brain Research, Meibergdreef 33, 1105 AZ Amsterdam, The Netherlands, [2]Department of Neurology, Leiden University Medical Center, 2300 RC Leiden, The Netherlands, [3]Laboratory of Pathology East Netherlands, 7512 AD Enschede, The Netherlands and [4]Department of Neurology, University Hospital Groningen, 9713 AW Groningen, The Netherlands

Received May 6, 2004; Revised and Accepted June 8, 2004

Polyglutamine diseases are characterized by neuronal intranuclear inclusions (NIIs) of expanded polyglutamine proteins, indicating the failure of protein degradation. UBB^{+1}, an aberrant form of ubiquitin, is a substrate and inhibitor of the proteasome, and was previously reported to accumulate in Alzheimer disease and other tauopathies. Here, we show accumulation of UBB^{+1} in the NIIs and the cytoplasm of neurons in Huntington disease and spinocerebellar ataxia type-3, indicating inhibition of the proteasome by polyglutamine proteins in human brain. We found that UBB^{+1} not only increased aggregate formation of expanded polyglutamines in neuronally differentiated cell lines, but also had a synergistic effect on apoptotic cell death due to expanded polyglutamine proteins. These findings implicate UBB^{+1} as an aggravating factor in polyglutamine-induced neurodegeneration, and clearly identify an important role for the ubiquitin–proteasome system in polyglutamine diseases.

INTRODUCTION

At least nine different neurodegenerative diseases are known that are caused by the expansion of a CAG repeat in the coding region of a transcribed gene, including the spinocerebellar ataxias (SCAs) and Huntington disease (HD) (1,2). All these CAG expansion diseases are characterized by progressive neuronal dysfunction starting during adult-life and resulting in severe neurodegeneration. In the channelopathy SCA6, neurodegeneration is caused by a small CAG expansion (to 19–30 repeats) in a calcium channel subunit that presumably causes a change of function (3). The other eight diseases are probably caused by a gain of function of the proteins carrying the expanded polyglutamine repeat. The pathological repeat length for these genuine polyglutamine expansion disorders starts around 40 glutamine repeats in the affected gene, with increasing severity and earlier manifestation upon greater expansion (1).

One of the hallmarks of the pathology of polyglutamine diseases is the formation of neuronal intranuclear inclusions (NIIs) in the affected areas of the brain (4). Although many of the proteins carrying the polyglutamine repeat have a cytoplasmic function, upon polyglutamine expansion they all form intranuclear inclusions that contain at least the expanded polyglutamine fragment. In HD, for instance, the NIIs contain only the N-terminal part of huntingtin with the polyglutamine stretch (4–7). The major pathological difference between the polyglutamine diseases is the regional distribution of neurodegeneration. In HD, the striatum is the most severely affected area and the cortex is affected to a lesser extent (8). In SCA3, in contrast, neuronal degeneration occurs primarily in the nuclei of the brainstem and the spinal cord (9). This regional specificity is probably caused by differences in expression levels of the respective disease genes among the various brain regions or different vulnerability of various types of neurons. In addition to the repeat expansion, other

*To whom correspondence should be addressed. Email: f.van.leeuwen@nih.knaw.nl

factors, such as proteasomal activity and expression or recruitment of cellular chaperones, probably influence polyglutamine toxicity and disease development (10–12).

NIIs contain ubiquitin or ubiquitinated proteins, which indicates that the aggregating proteins are targeted to, but not degraded by, the proteasome (4,13). Furthermore, *in vitro* studies have shown that expanded polyglutamines can directly inhibit the proteasome (14,15). In addition, in SCA3 patients, subunits of the 26S proteasome have been shown to be recruited to NIIs (16,17). Finally, in SCA1 transgenic mice, the Purkinje cell pathology was aggravated by mutation of the E6-AP ubiquitin ligase (18). All these findings point towards an involvement of the ubiquitin–proteasome system (UPS) in the pathogenesis of polyglutamine diseases and to an enhancement of neurodegeneration by further impairment of the UPS (19).

We previously reported that, in Alzheimer disease (AD), an aberrant form of ubiquitin (UBB^{+1}) accumulates in the neuropathological hallmarks of this disease (20). This UBB^{+1} protein is formed by a dinucleotide deletion (ΔGU), leading to a +1 reading frame in the mRNA, and subsequent translation to a protein with an aberrant C-terminus. Thus far UBB^{+1} protein has been found in the hallmarks of several neurodegenerative diseases, including AD and other tauopathies, whereas it was not detected in synucleinopathies and young control patients without pathology (20,21). The aberrant transcript, however, in contrast to the protein, appeared to be present even in young controls. Under normal circumstances, neurons can apparently cope with UBB^{+1}, and accumulation of this protein reflects proteasomal dysfunction in different neuropathological disorders (21).

In vitro studies have shown that, although UBB^{+1} can be degraded by the proteasome (21,22), at higher concentrations it inhibits proteasomal degradation of cellular proteins and leads to cell death in neuroblastoma cells (23,24). In addition, UBB^{+1} has been implicated recently to mediate neurodegeneration via downstream interaction with the E2-25K ubiquitin conjugating enzyme, which induces amyloid-β neurotoxicity *in vitro* (25). In this perspective, UBB^{+1} might accelerate disease progression and increase the severity of the disease. Notably, recent reports show that the proteasome activity is indeed decreased in AD (26,27), strengthening the idea that UBB^{+1} accumulation is intimately related to impairment of the proteasome (19).

Different findings point towards defective protein degradation in polyglutamine diseases. We examined post-mortem brain material of HD and SCA3 patients for the accumulation of UBB^{+1}, as a marker for proteasomal impairment. Moreover, we used a cellular model for polyglutamine disease to study the contribution of UBB^{+1} to disease progression, i.e. polyglutamine aggregation and cell death.

RESULTS

To identify NIIs in different brain areas of HD and SCA3 patients, we used antibodies against the N-terminal fragment of the huntingtin protein or full-length ataxin-3, respectively (Fig. 1A). In addition, we used an ubiquitin antibody and the 1C2 antibody to identify the inclusions. SCA6 showed staining of cytoplasmic aggregates with the α1A-subunit antibody (data not shown).

With antibodies against the UBB^{+1} protein, we detected immunopositive NIIs in the cortex (Fig. 1A) and striatum of all HD patients ($N = 30$). We found accumulation of UBB^{+1} not only in adult-onset patients but also in juvenile HD patients. Furthermore, we detected UBB^{+1} immunopositive NIIs in all SCA3 patients ($N = 6$), in all the areas investigated (Fig. 1A). Besides localization to the NIIs, we also found cytoplasmic staining for UBB^{+1} in the affected neurons of HD and SCA3 patients (Fig. 1A). In contrast, in the SCA6 patients ($N = 2$), we did not find any UBB^{+1} staining in the affected regions (data not shown). To ascertain whether UBB^{+1} localizes to all or only to a subset of NIIs stained with 1C2, we performed double immunofluorescent stainings on tissue sections of both HD and SCA3 patients. We found colocalization of polyglutamine proteins and UBB^{+1} in all the inclusions that were found in juvenile as well as adult-onset HD and in SCA3 (Fig. 1B). Accumulation of UBB^{+1} is thus not specific for HD, but a general phenomenon found in polyglutamine diseases.

Besides being a marker for proteasome impairment, *in vitro*, UBB^{+1} inhibits the proteasome (22,24). Constructs with expanded polyglutamine repeats can be used to mimic many of the features of polyglutamine diseases in cell lines, including aggregate formation and interaction with other proteins (18,28–30).

To investigate the impact of UBB^{+1} protein on aggregate formation, we used plasmids with a truncated huntingtin fragment containing 19, 38 or 43 glutamine repeats (HA–Q19–green fluroscent protein (GFP), HA–Q38–GFP and HA–Q43–GFP) in combination with plasmids containing either UBB^{+1} or a lysine mutant of UBB^{+1} ($UBB^{+1;K29,48R}$), which does not inhibit the proteasome (22). Co-transfection of UBB^{+1} with the normal Q19 polyglutamine length resulted in distribution of polyglutamine protein throughout the cells and cytoplasmic staining for UBB^{+1} (Fig. 2A). However, besides accumulation of UBB^{+1} in cells with expanded polyglutamine proteins we found colocalization with the inclusions of both the intermediate Q38 (Fig. 2B and C) and the expanded Q43 (Fig. 2D and E) polyglutamine proteins. The nuclear localization of the aggregates in these cells was similar to that observed in post-mortem brain material of the different polyglutamine diseases. In addition, a number of cells display a clear apoptotic morphology, with fragmented nuclei (Fig. 2C and E), in agreement with previous findings for UBB^{+1}, or expanded polyglutamines alone (23,30). In contrast to UBB^{+1}, after transfection with $UBB^{+1;K29,48R}$ we found no colocalization with the aggregating polyglutamines (Fig. 2F; Q43). It is remarkable that this latter ubiquitin mutant is not incorporated in the inclusions, although cytoplasmic levels are higher than that of UBB^{+1} transfected cells (22).

For functional characterizations we used neuronally differentiated human neuroblastoma cells (SH-SY5Y) (31). Cell-proliferation markedly influences the aggregate formation and cell death (32), which makes differentiated cells a more useful model for functional assays. In our experiments, HeLa cells showed comparable aggregate formation, but much lower levels of cell death due to proliferation and susceptibility (data not shown).

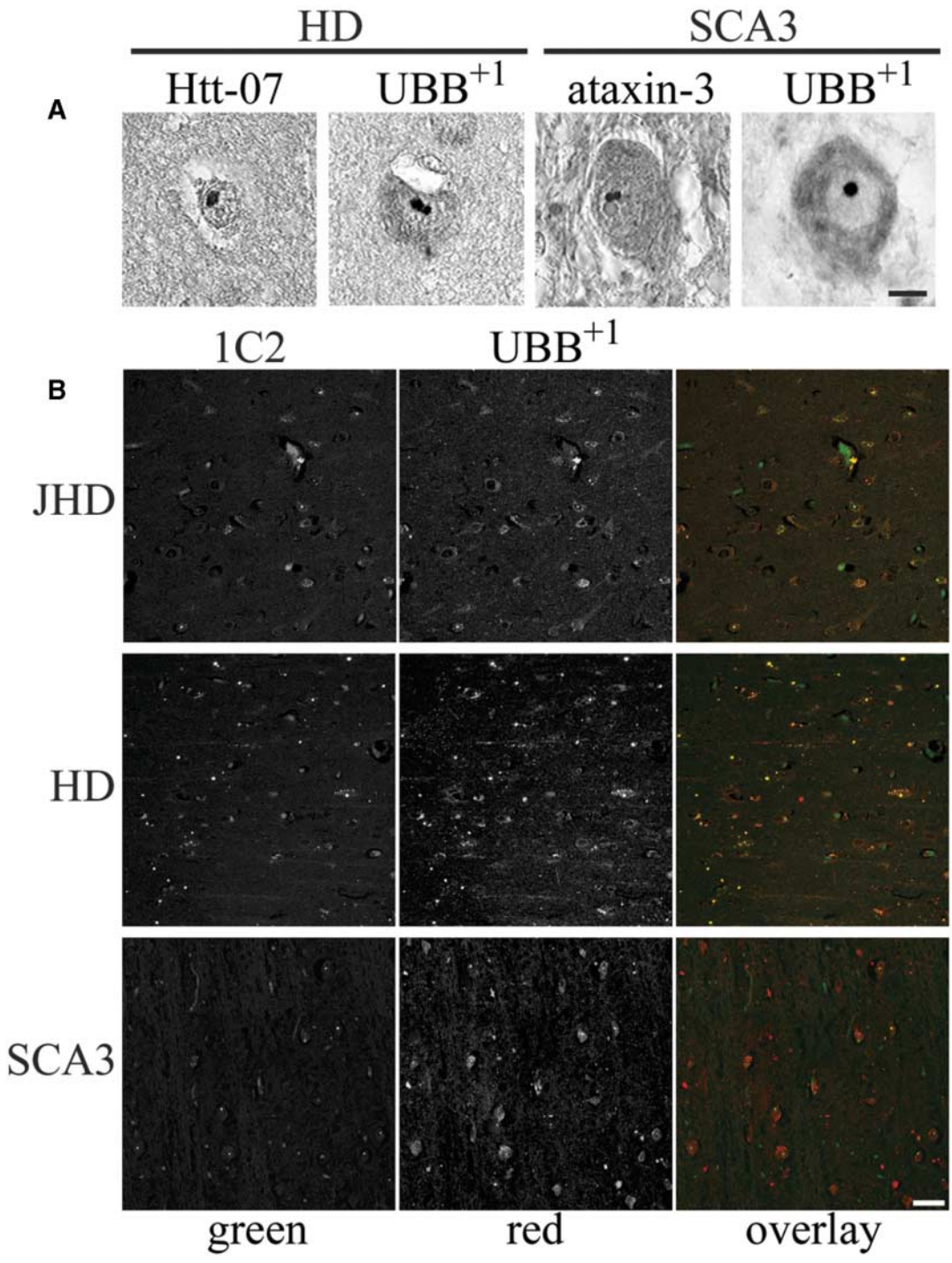

Figure 1. UBB^{+1} colocalizes with polyglutamine proteins in HD and SCA3. (**A**) Staining of paraffin sections of the frontal cortex of a HD patient and the pons of a SCA3 patient for UBB^{+1} and, respectively, Htt-07 and α-ataxin-3. Pictures show staining of NIIs with UBB^{+1}, distinct from the nucleoli, in both polyglutamine diseases. Magnification bar is 10 μm. (**B**) Double stainings show UBB^{+1} staining in all inclusions positive for 1C2 in juvenile as well as adult onset HD and in SCA3. Magnification bar is 50 μm. Note also the cytoplasmic staining for UBB^{+1} in both disorders, (A) and (B).

We quantified the aggregate formation after lentiviral transduction of SH-SY5Y neuroblastoma cells with polyglutamine vectors in combination with UBB^{+1} or the double lysine mutant of UBB^{+1} (Fig. 3A). The truncated huntingtin fragments with 38 or 43 glutamines show a marked increase in aggregate formation under the influence of UBB^{+1} in comparison with UBB$^{+1;K29,48R}$. Accumulation of UBB^{+1} causes an increase in polyglutamine protein and thus enhances the aggregate formation. For the huntingtin fragment with 38 glutamines, we even find a doubling of the number of aggregate

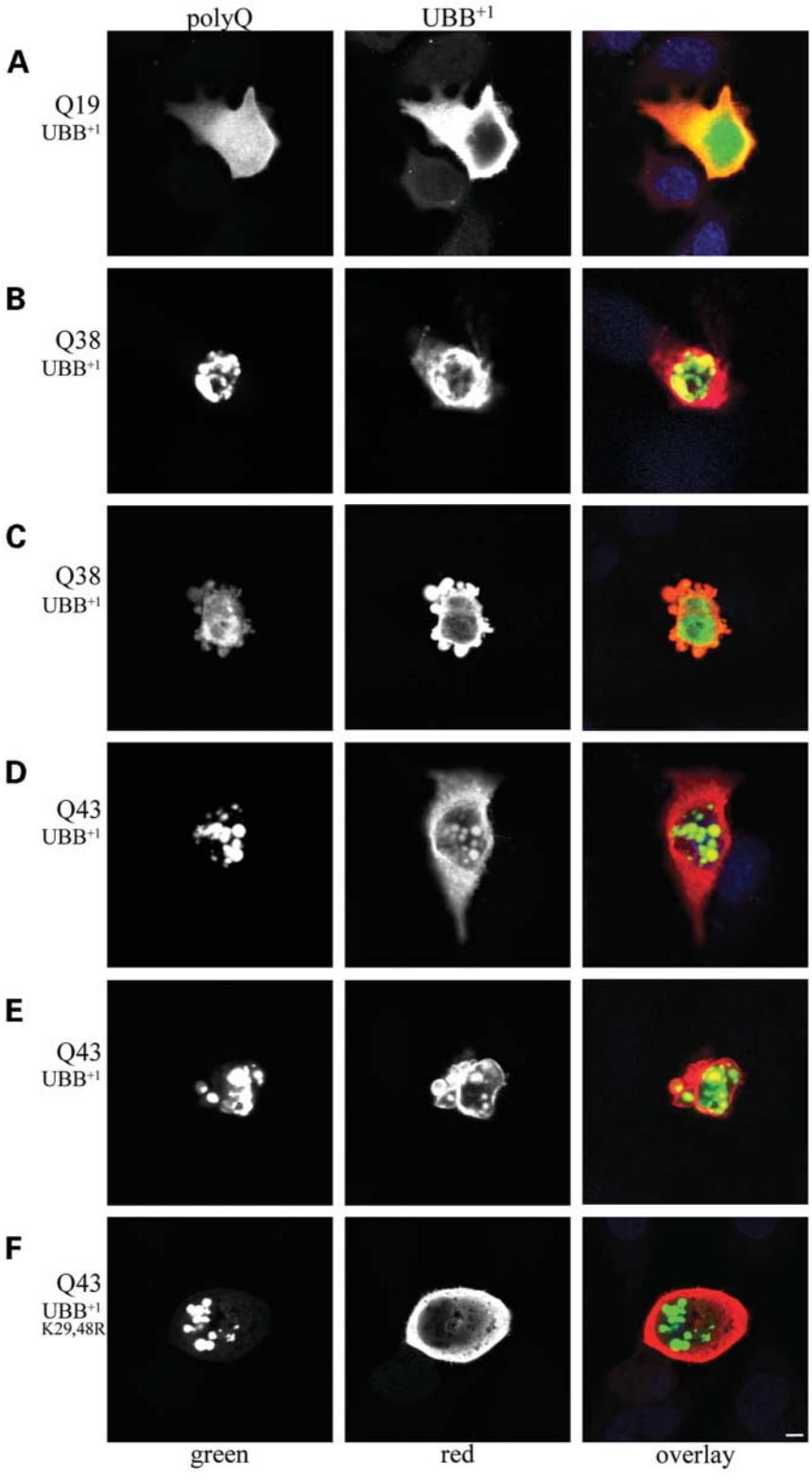

Figure 2. UBB^{+1} colocalizes with expanded polyglutamines *in vitro*. HeLa cells co-transfected with plasmids with a truncated huntingtin fragment containing 19, 38 or 43 glutamine repeats (HA–Q–GFP) together with constructs for UBB^{+1} or $UBB^{+1;K29,48R}$, were fixed 4 days post-transfection. All cells that were transfected with the construct containing 19 glutamines showed a diffuse cellular polyglutamine staining [(**A**), green; left panel]. Constructs with 38 and 43 glutamine repeats result in the formation of multiple polyglutamine aggregates [respectively, (**B**) and (**C**), and (**D**), (**E**) and (**F**); green; left column]. Co-transfection with UBB^{+1} gave cytoplasmic staining for UBB^{+1} (A)–(E) (in red; middle column) with all constructs. In addition, UBB^{+1} co-aggregates with the polyglutamine constructs Q38 (B and C) and Q43 (D and E), whereas $UBB^{+1;K29,48R}$ only shows cytoplasmic staining despite aggregate formation of Q43 (F). The right column shows the overlay of UBB^{+1} and polyglutamine, with faint To-Pro nuclear staining in blue. Magnification bar is 10 μm.

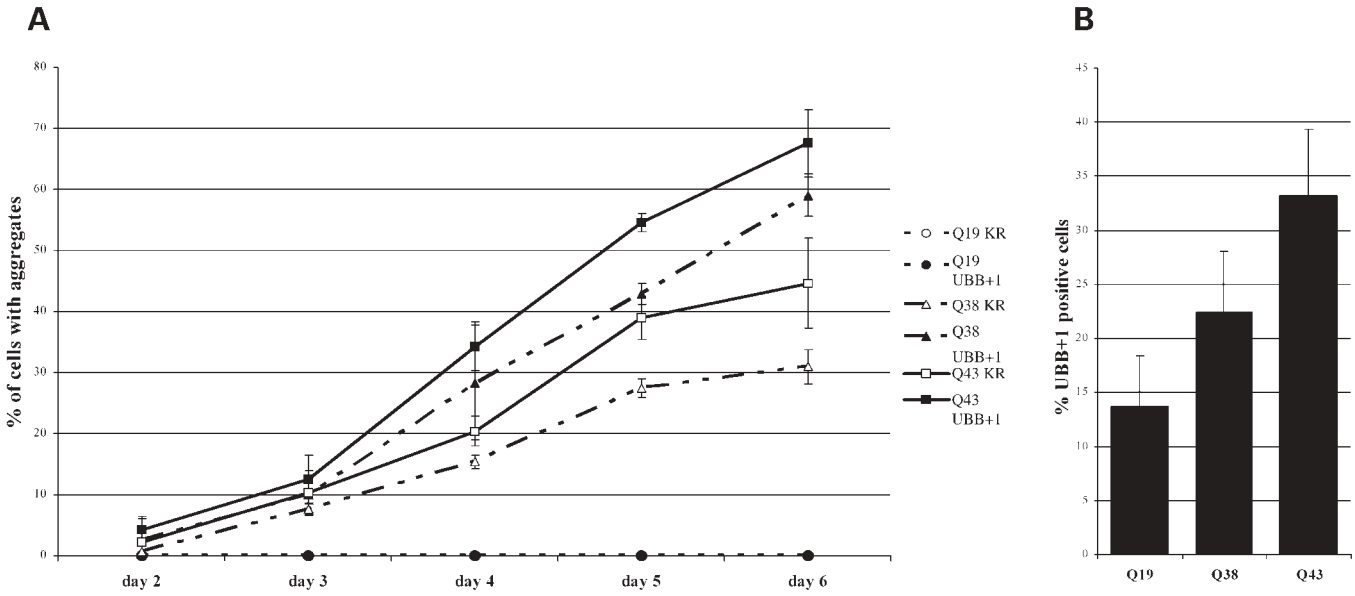

Figure 3. UBB^{+1} induces aggregate formation and preferentially accumulates with expanded polyglutamines. Differentiated SH-SY5Y neuroblastoma cells were lentivirally infected with constructs with truncated huntingtin fragments containing 19, 38 or 43 glutamine repeats (HA–Q–GFP) in combination with either $UBB^{+1;K29,48R}$ (KR) or UBB^{+1} (+1). Cells were quantified for aggregate formation every 24 h after infection (**A**). Note that huntingtin with 19 glutamines does not result in the formation of aggregates, resulting in two overlapping lines in this graph. Constructs with 38 and 43 glutamines both show a marked increase in the number of aggregate forming cells in the presence of UBB^{+1}, as represented by the two uppermost lines. Statistical analysis by three-way ANOVA demonstrated a strong correlation between the aggregate formation of expanded polyglutamines, the influence of UBB^{+1} and the time course ($P < 0.001$). Expression of UBB^{+1} was quantified 4 days after infection (**B**). The expression of expanded huntingtin fragments causes a preferential accumulation of UBB^{+1} in these cells. Statistical analysis by one-way ANOVA showed a highly significant correlation between repeat expansion of the huntingtin fragments and the UBB^{+1} accumulation ($P = 0.001$). All experiments were performed in triplicate.

forming cells due to UBB^{+1} from 4 days onwards (Fig. 3A). Statistical analysis by three-way analysis of variance (ANOVA) confirmed a highly significant correlation between the aggregate formation, the influence of UBB^{+1} and the time course ($P < 0.001$). Immunofluorescent stainings furthermore show a preferential accumulation of UBB^{+1} in the cells with the expanded huntingtin fragments (Fig. 3B). Quantification of the cells 4 days after infection showed a clear increase in the amount of UBB^{+1} expressing cells upon expansion of the polyglutamine repeat (Fig. 3B). Statistical analysis by one-way ANOVA confirmed a significant correlation between the repeat expansion and UBB^{+1} accumulation ($P = 0.001$).

We made cell lysates 6 days after infection and analyzed these by western blotting (Fig. 4). Western blots probed with an anti-HA antibody showed, owing to UBB^{+1}, a 3-fold increase in sodium dodecyl sulfate (SDS)-insoluble aggregate fraction at the top of the gel with both 38 and 43 glutamines (Fig. 4A). The amount of soluble polyglutamine protein, however, shows only a slight increase for all repeat lengths (Fig. 4B). The bars (Fig. 4D) represent the relative amount of aggregates (Fig. 4A) after correction for β-actin (Fig. 4C). Statistical analysis by two-way ANOVA confirmed that UBB^{+1} has a pronounced, highly significant synergistic effect on the aggregate formation of constructs with 38 and 43 glutamines ($P < 0.001$).

To investigate the effect of the expression of the different proteins on the viability of neuroblastoma cells, we performed a cell survival assay (Fig. 5). The scatter plots show a representative FACS analysis of the polyglutamine expressing cells (Fig. 5A). Dead cells show a marked increase in red-fluorescence due to conversion of the reactive dye (higher population). Cell death due to Q19 represents the background level of cell death due to infection and culturing of the cells, whereas Q19 itself is not toxic (28). Combination of Q19 with $UBB^{+1;K29,48R}$, which was used as a control, does not affect cell death. Expansion of the polyglutamine repeat resulted in a moderate increase in cell death when combined with $UBB^{+1;K29,48R}$. We measured a small but significant increase for the plasmid with 38 glutamines, whereas the expansion to 43 glutamines caused a significant 3-fold increase in cell death. Upon addition of UBB^{+1}, a moderate and significant increase in cell death was found for the Q19 construct. In contrast to previous experiments (23), lentiviral transduction resulted in only moderate cell death for UBB^{+1} (Fig. 4B) due to degradable levels of UBB^{+1} protein (21). However, UBB^{+1} in combination with longer glutamine repeats caused a much more pronounced increase in cell death for Q38 as well as for Q43 constructs. Statistical analysis by two-way ANOVA confirmed that the combination of UBB^{+1} with constructs of 38 and 43 glutamines has a pronounced, highly significant synergistic effect on the cell death mechanism ($P < 0.001$). This synergistic effect manifests itself as an increase of the absolute effect of UBB^{+1} on cell death with increasing length of the huntingtin fragment. Caspase inhibition by Ac-DEVD-CHO resulted in a marked decrease in cell death in our polyglutamine model, indicating that cell death due to UBB^{+1} as well

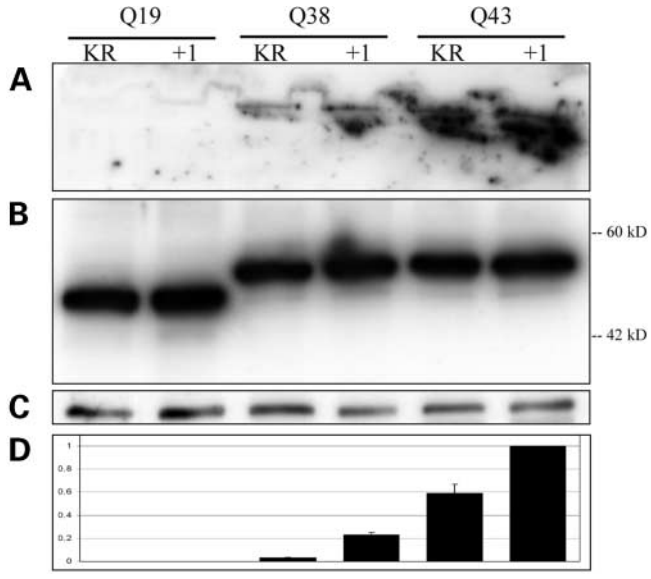

Figure 4. UBB^{+1} increases aggregate formation of expanded polyglutamines. Differentiated SH-SY5Y neuroblastoma cells were lentivirally infected with constructs with truncated huntingtin fragments containing 19, 38 or 43 glutamine repeats (HA–Q–GFP) in combination with either $UBB^{+1;K29,48R}$ (KR) or UBB^{+1} (+1), and harvested 6 days after infection. (**A**) Especially with 38 glutamines a marked increase is seen in the SDS-insoluble aggregate fraction that is retained at the top of the gel when cells are co-infected with UBB^{+1}. The irregular appearance of the SDS-insoluble fraction is caused by the intrinsic property of the aggregates that hardly run into the stacking-gel of the western blot. (**B**) The levels of soluble polyglutamine protein show a minor increase (around 60 kDa). (**C**) β-Actin staining as a loading control. (**D**) Bars show the relative integrated optical densities of the aggregate fraction after correction for loading. Statistical analysis by two-way ANOVA showed a strong synergistic effect of UBB^{+1} on aggregate formation by expanded polyglutamines ($P < 0.001$). All experiments were performed in triplicate.

as due to expanded polyglutamines occurs via an apoptotic pathway (Fig. 4B). The percentage of cell death with caspase inhibitor did not significantly increase above the background level.

DISCUSSION

Previously we reported that the accumulation of UBB^{+1} in tauopathies is a marker for proteasomal dysfunction (21). Here, we show that this accumulation is not only indicative of proteasome impairment, but that UBB^{+1} apparently also contributes to the pathogenesis of polyglutamine diseases. The accumulation of UBB^{+1} protein enhances aggregate formation in a cellular model of polyglutamine disease. In addition, the toxicity of UBB^{+1} in combination with expanded polyglutamines is not just additive but clearly works synergistically. It thus suggests that both toxic proteins somehow intervene with the same or analogous pathways to compromise cellular function, and eventually cause cell death.

Molecular misreading of the UBB gene is a general process that occurs both in neurological diseases and in control individuals (21). We performed a ligase chain reaction (LCR), as described earlier (21), to confirm the presence of $UBB^{\Delta GU}$ transcripts in the mRNA from frontal cortex tissue of three different HD patients (data not shown). The GU deletion was present in all HD patients tested, indicating that at the level of the mRNA there is no difference between HD patients, non-demented controls or any of the previously tested neurological diseases (21). Differences in UBB^{+1} staining are probably the result of decreased proteasomal activity due to disease-related proteins or ageing (5,21,26,27,33). Neurological diseases such as Parkinson disease, in which impairment of the proteasome is not demonstrated, do not lead to UBB^{+1} accumulation (21,34).

Both HD and SCA3 form NIIs, and we demonstrated here that, independent of their protein context (huntingtin and ataxin-3, respectively) these aggregates contain UBB^{+1} (Fig. 1). Moreover, UBB^{+1} not only localizes to the inclusions; the cytoplasmic immunoreactivity for this aberrant protein is increased as well (Fig. 1A), indicating high protein levels that potentially impair the proteasome. Accumulation of UBB^{+1} reflects *in vivo* proteasomal impairment in the polyglutamine disorders, which is in agreement with previous *in vitro* results (14–16). What is striking is the accumulation of UBB^{+1} in all tested HD and SCA3 patients, irrespective of polyglutamine length and age, showing that UBB^{+1} can already accumulate at a young age (Fig. 1B). The high stability of ubiquitinated UBB^{+1} contributes to the accumulation in neurodegenerative disease, and it has been suggested that even low levels of misreading can result in toxic protein levels (24). We did not find UBB^{+1} in SCA6, suggesting proper functioning of the proteasome in this channelopathy. Indeed, the proteasome has not been implicated in disease progression in SCA6, and the inclusions, which are only present in the cytoplasm, are not ubiquitinated (35).

Although the mechanism by which different cellular proteins are recruited into NIIs is unknown, the presence of UBB^{+1} in NIIs in human tissue and in a cellular model implicates a similar mechanism. Accumulation of UBB^{+1} will probably start in the cytoplasm, followed by translocation into the NIIs. Interestingly, we showed that ubiquitination on lysine 29 or 48 is not only required for degradation of UBB^{+1}, in agreement with previous results (22), but is also needed for its translocation to the inclusions. Polyubiquitin chains of targeted proteins are bound to the S6a regulatory subunit of the 19S cap, and it is likely that both the UBB^{+1} resistance to degradation and its proteasomal impairment resemble binding to this subunit, but lack of processing through the 20S core (24,36). Components of the proteasome, and especially the 19S cap structure, have been shown to be present in NIIs and could thus explain the localization of UBB^{+1} into the inclusions (16,17).

In addition to human brain material, we also found accumulation and co-aggregation of the proteasome substrate UBB^{+1} with expanded polyglutamines in a cellular model (Fig. 2). Moreover, the proteasome inhibitor UBB^{+1} causes an increase in aggregate formation of expanded polyglutamines (Figs 3A and 4). The expanded polyglutamine proteins reciprocally result in the preferential accumulation of UBB^{+1} in these cells (Fig. 3B). We suggest that inhibition of the degradation machinery is central to the development of polyglutamine diseases and causes accumulation of different aberrant proteins.

We demonstrated that, UBB^{+1} not only increases aggregate formation, but also has a synergistic effect on apoptotic cell-death by expanded polyglutamines (Fig. 5). Ubiquitinated

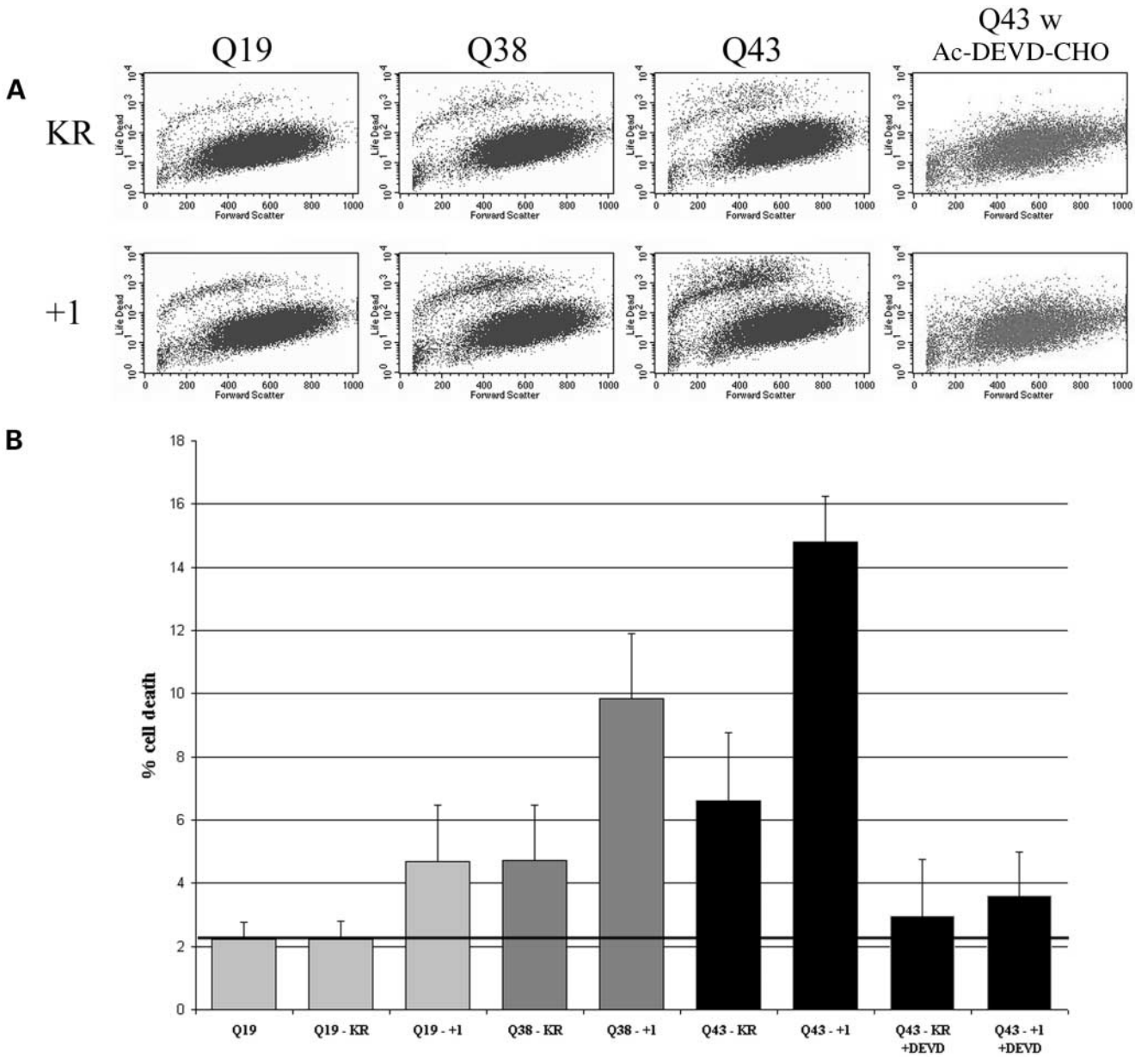

Figure 5. UBB^{+1} synergistically aggravates polyglutamine-induced cell death. Cell death of differentiated SH-SY5Y neuroblastoma cells, as assessed by a cell survival assay 6 days after infection, with constructs with 19, 38 or 43 glutamines (HA–Q–GFP) in combination with $UBB^{+1;K29,48R}$ (KR) as a control or UBB^{+1} (+1). (**A**) Polyglutamine–GFP positive cells were analyzed by flow cytometry for conversion of red-fluorescent dye (representative FACS analysis). Scatter plots clearly show the differential distribution of living cells (lower population) and dead cells (higher population; bright red-fluorescent). (**B**) The bars show the percentage of cell death that was observed under different conditions. Q19 shows the background percentage of cell death due to infection or culturing and no increase was observed in combination with $UBB^{+1;K29,48R}$ (B). The horizontal line signifies the percentage of background cell death. A minor increase in cell death was observed with expansion of the polyglutamine repeat. Co-infection with UBB^{+1} caused a small increase in cell death of Q19, but a marked increase was observed with constructs of both 38 and 43 glutamines. Statistical analysis by two-way ANOVA indeed showed a strong synergistic effect of UBB^{+1} on cell death by expanded polyglutamines ($P < 0.001$). Caspase inhibition with Ac-DEVD-CHO resulted in a marked decrease of cell death due to UBB^{+1} as well as due to expanded polyglutamines. Statistical analysis revealed no significant increase in cell death in comparison with the background level. All experiments were performed in triplicate.

UBB^{+1} and expanded polyglutamine proteins have been shown to inhibit the proteasome *in vitro* (14,15,22), and we demonstrated here that both factors enhance the effect of the other aberrant protein. The mutual decrease of proteasome activity probably leads to further accumulation of aberrant proteins, and eventually cell death. The fact that ubiquitination of UBB^{+1} is required for its proteasomal inhibition (22), its toxicity (23) and its contribution to aggregate formation and polyglutamine-induced cell death suggests that polyubiquitination is a prerequisite for both aggregate formation and cell death.

Although the genetic basis of polyglutamine diseases is known, a number of questions remain unanswered as to the

precise cause of toxicity and whether aggregates are either beneficial or toxic (37). Even between individuals with similar repeat length, there are differences as to the age at onset, the progression, and the extent of atrophy (1,8,38,39). Recent reports indicate that genetic and familial factors account for a great deal of variation of the age at onset in HD (12,40). Possible candidates include proteasome subunits and cellular chaperones (10,11) and, as described in the present paper, also factors such as UBB^{+1} can act as modifiers of both the onset and severity of the disease.

From the present study it is evident that UBB^{+1} not only accumulates in polyglutamine diseases, indicating impairment of the proteasome, but probably plays a role in neurodegeneration itself. In addition to co-aggregation with polyglutamine proteins, ubiquitinated UBB^{+1} synergistically aggravates polyglutamine-induced aggregate formation, and especially cell death. Targeting of UBB^{+1} to the proteasome by ubiquitination is thereby required for degradation, toxicity and colocalization with the NIIs. Consequently, the accumulation of UBB^{+1} in HD and SCA3 post-mortem tissue, in both the inclusions and the cytoplasm of neurons, implicates UBB^{+1} as an aggravating factor in polyglutamine-induced neurodegeneration, and clearly identifies an important role for the UPS in polyglutamine diseases. These results indicate that proteasomal activation or removal of its blockades is a promising avenue for the treatment of polyglutamine diseases.

MATERIALS AND METHODS

Patients

Autopsy material was obtained from the Huntington bank (Leiden University Medical Center, The Netherlands) for HD cases, and the Laboratory of Pathology East Netherlands (Enschede, The Netherlands) and University Hospital Groningen (Groningen, The Netherlands) for SCA cases (Table 1). We analyzed striatal tissue from four different HD patients and frontal cortex tissue of 30 HD patients with polyglutamine expansion of various lengths. Furthermore, we examined the hippocampus, pons, mesencephalon and medulla oblongata of six different SCA3 patients and the hippocampus and cerebellum of two SCA6 patients. All brain areas were fixed in formaldehyde and subsequently embedded in paraffin.

Immunohistochemistry

Paraffin sections (6 μm) were immunohistochemically labeled with different antibodies using the peroxidase–anti-peroxidase method with nickel intensification as described previously (20). The 1C2 monoclonal antibody against expanded polyglutamine repeats (1:10 000; Chemicon, Temecula, USA) (41), polyclonal Htt-07 antiserum against the N-terminus of huntingtin (1:100) (7), polyclonal anti-ataxin-3 antibody (1:2000) (42) and polyclonal A6RPT-C against the C-terminus of the α1A-subunit of the voltage-dependent calcium channel (1:100) (35) were used for the detection of the respective disease proteins. UBB^{+1} was detected using antisera against the C-terminal part of the protein [Ubi2A, 1:1000, bleeding 020698 and Ubi2 + 1, 1:1000, bleeding 010994; see literature for details on epitope and specificity (20,21)].

For double stainings, we subjected paraffin sections to irradiation with a broad spectrum lamp for at least 24h to reduce autofluorescence (43,44). We then deparaffinized sections and incubated them with the first antibodies overnight in a humid chamber at 4°C. We enhanced the UBB^{+1} signal using the avidin–biotin–complex (Vector Laboratories, Burlingame, USA) and tyramine procedure (45) (Sigma–Aldrich, St Louis, USA) and stained with streptavidin-conjugated-Cy5 (Jackson Laboratories, West Grove, USA). 1C2 was directly visualized using donkey-anti-mouse-Cy2. Signal specificity was demonstrated by swapping fluorescent dyes and omission of primary antibodies to exclude aspecific staining or signal enhancement. Images were obtained using a confocal laser scanning microscope (Zeiss 510).

Cell lines

HeLa cells were cultured in low-glucose Dulbecco's modified Eagle medium containing 10% fetal calf serum (FCS), supplemented with 100 U/ml penicillin and 100 μg/ml streptomycin (all Invitrogen, Grand Island, NY). Cells were cultured on 0.2% gelatin-coated glass coverslips in 24-well plates (Nunc, Roskilde, Denmark) 1 day before transfection.

SH-SY5Y neuroblastoma cells (ATCC:CRL-2260) were cultured in high-glucose Dulbecco's modified Eagle medium containing 15% FCS, supplemented with 100 U/ml penicillin and 100 μg/ml streptomycin (all Invitrogen). Cells were cultured in 6-well plates (Nunc) 1 day before infection.

Transfections

We performed transfections with the calcium-chloride method, using 0.5 μg plasmid DNA of each of the respective plasmids for 24-well plates (46). Polyglutamine plasmids containing a truncated huntingtin fragment with different polyglutamine repeats (19,38,43) flanked by a HA tag and GFP reporter sequence were provided by Dr de Christofaro (28). Vectors for ubiquitin, UBB^{+1} and a lysine mutant of UBB^{+1} in which both lysine 29 and 48 are mutated into an arginine residue ($UBB^{+1;K29,48R}$) were described earlier (22).

Cells were fixed 4 days after transfection and stained for UBB^{+1} [Ubi3, 1:500, bleeding 050897 (23)]. Subsequently cells were incubated with donkey-anti-rabbit-Cy3 (1:200; Jackson Laboratories) and ToPro-3 nuclear staining (1:200, Molecular Probes, Leiden, The Netherlands). After staining for UBB^{+1}, pictures were obtained using a confocal laser scanning microscope (Zeiss 510).

Infections

cDNAs for UBB^{+1}, $UBB^{+1;K29,48R}$, HA–Q19–GFP, HA–Q38–GFP and HA–Q43–GFP were cloned in the lentiviral transfer plasmid pRRLsin-PPThCMV-GFP-pre (46). VSV-G pseudotyped lentivirus was produced by co-transfection of the transfer plasmid and helper plasmids (pCMVdeltaR8.74 and pMD.G.2) in 293T cells. Medium was harvested 24 and 48 h after transfection and concentrated by ultracentrifugation.

Table 1. Clinicopathological information of Huntington, SCA3 and SCA6 patients

Patient number	Age	Sex	Postmortem delay (h)	Brain weight (g)	Fixation duration (days)	CAG repeat expansion	Vonsattel grade	Areas investigated
HD[a]								
1	11	F	21	1240	21	22–84	3	Frontal cortex
2	20	F	36	860	21	17–86	4	Frontal cortex
3	33	F	144	1220	122	20–52	3	Frontal cortex
4	39	M	10	NA	363	15–59	4	Frontal cortex, striatum
5	40	M	16	1400	124	10–41	3	Frontal cortex
6	41	F	24	1150	42	16–46	3	Frontal cortex, striatum
7	49	M	120	1120	186	21–51	4	Frontal cortex
8	49	F	NA	NA	186	17–47	3	Frontal cortex
9	50	M	4	1230	31	20–47	3	Frontal cortex
10	51	M	4	1260	2	27–45	3	Frontal cortex
11	51	F	5	900	14	19–46	4	Frontal cortex
12	51	F	74	1100	NA	15–43	3	Frontal cortex
13	52	F	20	840	31	16–53	4	Frontal cortex
14	55	M	24	1250	124	22–47	2–3	Frontal cortex
15	56	M	32	1250	2	18–49	3	Frontal cortex
16	57	F	72	1200	162	16–43	3	Frontal cortex
17	58	F	34	1170	7	24–43	3	Frontal cortex
18	60	M	12	1200	248	20–43	3	Frontal cortex
19	60	M	NA	NA	35	26–47	4	Frontal cortex
20	61	F	17	1050	NA	17–45	3	Frontal cortex
21	61	F	24	840	21	21–47	4	Frontal cortex
22	62	M	12	1200	62	20–43	3	Frontal cortex
23	63	F	10	1100	58	17–45	3	Frontal cortex, striatum
24	64	F	60	1080	7	19–42	3	Frontal cortex
25	66	M	28	1125	78	21–40	3–4	Frontal cortex
26	66	F	NA	950	107	20–44	3–4	Frontal cortex, striatum
27	68	F	12	1130	62	20–42	3	Frontal cortex
28	69	F	24	NA	155	21–40	3	Frontal cortex
29	69	M	48	1200	62	16–42	3	Frontal cortex
30	76	M	14	970	81	15–46	3	Frontal cortex
SCA3[a]								
31	34	M	NA	1598	28	20–75		Medulla oblongata
32	51	M	24	1244	21	27–72		Hippocampus, mesencephalon
33	59	F	12	1290	21	20–72		Hippocampus, pons
34	62	M	21	1236	21	23–70		Hippocampus, pons
35[c]	65	M	<12	1258	28	27–72		Pons
36[c]	66	M	14	1220	21	24–70		Pons
SCA6[a]								
37	69	M	46	1395	28	[b]		Hippocampus, cerebellum
38	76	M	24	1418	120	22		Cerebellum

[a]All cases positive with htt-07, ataxin-3 and A6RPT-C, respectively.
[b]Not available, but most probably 21 or 22.
[c]Brothers.
NA, not available.

Virus pellets were resuspended in phosphate buffered saline (PBS) containing 0.5% bovine serum albumin (BSA) (Sigma). Stocks were titered with a HIV-1 p24 coat protein ELISA (NEN Research, Boston, USA). Lentiviral vectors were used to infect SH-SY5Y neuroblastoma cells at a multiplicity of infection of 50.

Quantification of cells

For aggregate formation, cells were counted manually every 24 h after infection. The percentage of polyglutamine expressing cells with aggregates was quantified over three randomly selected fields per experiment. Experiments were performed in triplicate and statistics was performed using three-way ANOVA, testing the interaction between repeat expansion, UBB^{+1} protein expression and time course.

UBB^{+1} immunopositive cells, were counted after fixation and immunofluorescent staining for UBB^{+1}. The percentage of polyglutamine expressing cells positive for UBB^{+1} was quantified over three randomly selected fields per experiment. Experiments were performed in triplicate and statistics was done using one-way ANOVA, testing the significance of repeat expansion on UBB^{+1} accumulation.

Western blots

We harvested neuroblastoma cells (SH-SY5Y) 6 days after infection in cold PBS. Cell pellets were resuspended in

lysis-buffer (1% NP40, 0.1 M NaCl, 0.01 M Tris–HCl pH 8.0, 1 mM EDTA pH 8.0) containing protease inhibitors; 1 mM PMSF and 10 μg/ml leupeptin. We performed cell lysis at 4°C for 30 min and passed samples through a 25G needle to ensure complete lysis. All samples were loaded onto SDS–PAGE gels and transferred semi-dry onto nitrocellulose (Schleicher and Schuell, Dassel, Germany). Polyglutamine proteins were detected using a monoclonal antibody directed against the HA tag (12CA5, 1:100, culture supernatant) (47). Blots were additionally probed with a monoclonal β-actin antibody (JLA2.0, 1:500; Developmental Studies Hybridoma Bank, Iowa, USA) as a control for the amount of cell-lysate loaded. Subsequently, blots were incubated with anti-mouse HRP (1:1000; DAKO, Glostrup, Denmark) followed by Lumilight ECL (Perkin Elmer, Norwalk, USA) chemiluminescence. The integrated optical density of the bands was determined by image analysis with Image Pro Plus and after correction for β-actin the value for Q43 with UBB^{+1} was set to 1 to obtain the relative ratios.

Cell survival assay

We assessed SH-SY5Y cell survival using a Life-Dead® kit (red-fluorescence; Molecular Probes, Leiden, The Netherlands) and analyzed the cells on a flow cytometer (Becton Dickinson, Palo Alto, USA) according to the manufacturers protocol. In short, we harvested lentivirally infected cells (see before) 6 days after infection using 0.25% trypsin (Invitrogen), washed in PBS and incubated them for 30 min with the fluorescent reactive dye. Subsequently, we fixed cells with 4% formaldehyde for 15 min and resuspended in PBS–BSA (1 × PBS pH 7.6, 0.5% BSA, 0.1% NaN_3). We analyzed polyglutamine–GFP expressing cells by flow cytometry for conversion of the Life-Dead® kit reactive dye. At least 10^4 polyglutamine–GFP positive cells were examined per sample. Dead cells showed a marked increase of red-fluorescence over living cells due to conversion of the dye (Fig. 4A). Experiments were performed in triplicate and statistics were done using two-way ANOVA, testing the interaction between UBB^{+1} protein expression and repeat expansion. Caspase inhibition was performed by addition of 100 μM Ac-DEVD-CHO (Sigma) to the culture medium every 2 days.

ACKNOWLEDGEMENTS

We thank Drs T. de Christofaro (Universita di Napoli 'Federico II', Naples, Italy) for sending of polyglutamine plasmids, L. Naldini (Institute for Cancer Research, University of Torino Medical School, Italy) for lentiviral plasmids, H.L. Paulson (University of Iowa, Iowa, USA) for the ataxin-3 antibody, K. Ishikawa (Medical and Dental University, Bunkyo-ku, Japan) for A6RPT-C staining, M. Losekoot (Molecular Genetics Laboratory, Leiden, The Netherlands) for CAG determinations, N. Dantuma (Karolinska Institutet, Stockholm, Sweden) and Department of Experimental Internal Medicine (Amsterdam Medical Center, Amsterdam, The Netherlands) for technical advice and use of FACS equipment, J.A. Sluijs (Netherlands Institute for Brain Research, Amsterdam, The Netherlands) for virus production, J.J. van Heerikhuize and R.F. Roelofs (Netherlands Institute for Brain Research, Amsterdam, The Netherlands) for technical advice, W. Verweij (Netherlands Institute for Brain Research, Amsterdam, The Netherlands) and J.M. Ruijter (University of Amsterdam, Amsterdam, The Netherlands) for critical remarks and statistical advice. Financial support was given by the Prinses Beatrix Foundation (MAR 99-0113), the 5th Framework 'Quality of life and management of living resources' EU grant (QLRT-1999-02238), Hersenstichting Nederland (Grant H00.06) and Platform Alternatieven voor Dierproeven (#98-19).

REFERENCES

1. Zoghbi, H.Y. and Orr, H.T. (2000) Glutamine repeats and neurodegeneration. *Annu. Rev. Neurosci.*, **23**, 217–247.
2. Nakamura, K., Jeong, S.Y., Uchihara, T., Anno, M., Nagashima, K., Nagashima, T., Ikeda, S., Tsuji, S. and Kanazawa, I. (2001) SCA17, a novel autosomal dominant cerebellar ataxia caused by an expanded polyglutamine in TATA-binding protein. *Hum. Mol. Genet.*, **10**, 1441–1448.
3. Zhuchenko, O., Bailey, J., Bonnen, P., Ashizawa, T., Stockton, D.W., Amos, C., Dobyns, W.B., Subramony, S.H., Zoghbi, H.Y. and Lee, C.C. (1997) Autosomal dominant cerebellar ataxia (SCA6) associated with small polyglutamine expansions in the alpha 1A-voltage-dependent calcium channel. *Nat. Genet.*, **15**, 62–69.
4. DiFiglia, M., Sapp, E., Chase, K.O., Davies, S.W., Bates, G.P., Vonsattel, J.P. and Aronin, N. (1997) Aggregation of huntingtin in neuronal intranuclear inclusions and dystrophic neurites in brain. *Science*, **277**, 1990–1993.
5. Zhou, H., Cao, F., Wang, Z., Yu, Z.X., Nguyen, H.P., Evans, J., Li, S.H. and Li, X.J. (2003) Huntingtin forms toxic NH2-terminal fragment complexes that are promoted by the age-dependent decrease in proteasome activity. *J. Cell Biol.*, **163**, 109–118.
6. Sieradzan, K.A., Mechan, A.O., Jones, L., Wanker, E.E., Nukina, N. and Mann, D.M. (1999) Huntington's disease intranuclear inclusions contain truncated, ubiquitinated huntingtin protein. *Exp Neurol.*, **156**, 92–99.
7. Maat-Schieman, M.L., Dorsman, J.C., Smoor, M.A., Siesling, S., Van Duinen, S.G., Verschuuren, J.J., den Dunnen, J.T., Van Ommen, G.J. and Roos, R.A. (1999) Distribution of inclusions in neuronal nuclei and dystrophic neurites in Huntington disease brain. *J. Neuropathol. Exp. Neurol.*, **58**, 129–137.
8. Halliday, G.M., McRitchie, D.A., Macdonald, V., Double, K.L., Trent, R.J. and McCusker, E. (1998) Regional specificity of brain atrophy in Huntington's disease. *Exp. Neurol.*, **154**, 663–672.
9. Takiyama, Y., Oyanagi, S., Kawashima, S., Sakamoto, H., Saito, K., Yoshida, M., Tsuji, S., Mizuno, Y. and Nishizawa, M. (1994) A clinical and pathologic study of a large Japanese family with Machado-Joseph disease tightly linked to the DNA markers on chromosome 14q. *Neurology*, **44**, 1302–1308.
10. Willingham, S., Outeiro, T.F., DeVit, M.J., Lindquist, S.L. and Muchowski, P.J. (2003) Yeast genes that enhance the toxicity of a mutant huntingtin fragment or alpha-synuclein. *Science*, **302**, 1769–1772.
11. Chan, H.Y.E., Warrick, J.M., Andriola, I., Merry, D. and Bonini, N.M. (2002) Genetic modulation of polyglutamine toxicity by protein conjugation pathways in Drosophila. *Hum. Mol. Genet.*, **11**, 2895–2904.
12. Wexler, N.S., Lorimer, J., Porter, J., Gomez, F., Moskowitz, C., Shackell, E., Marder, K., Penchaszadeh, G., Roberts, S.A., Gayan, J. *et al.* (2004) Venezuelan kindreds reveal that genetic and environmental factors modulate Huntington's disease age of onset. *Proc. Natl Acad. Sci. USA*, **101**, 3498–3503.
13. Paulson, H.L., Perez, M.K., Trottier, Y., Trojanowski, J.Q., Subramony, S.H., Das, S.S., Vig, P., Mandel, J.L., Fischbeck, K.H. and Pittman, R.N. (1997) Intranuclear inclusions of expanded polyglutamine protein in spinocerebellar ataxia type 3. *Neuron*, **19**, 333–344.
14. Bence, N.F., Sampat, R.M. and Kopito, R.R. (2001) Impairment of the ubiquitin-proteasome system by protein aggregation. *Science*, **292**, 1552–1555.

15. Verhoef, L.G., Lindsten, K., Masucci, M.G. and Dantuma, N.P. (2002) Aggregate formation inhibits proteasomal degradation of polyglutamine proteins. *Hum. Mol. Genet.*, **11**, 2689–2700.
16. Chai, Y., Koppenhafer, S.L., Shoesmith, S.J., Perez, M.K. and Paulson, H.L. (1999) Evidence for proteasome involvement in polyglutamine disease: localization to nuclear inclusions in SCA3/MJD and suppression of polyglutamine aggregation *in vitro*. *Hum. Mol. Genet.*, **8**, 673–682.
17. Schmidt, T., Lindenberg, K.S., Krebs, A., Schols, L., Laccone, F., Herms, J., Rechsteiner, M., Riess, O. and Landwehrmeyer, G.B. (2002) Protein surveillance machinery in brains with spinocerebellar ataxia type 3: redistribution and differential recruitment of 26S proteasome subunits and chaperones to neuronal intranuclear inclusions. *Ann. Neurol.*, **51**, 302–310.
18. Cummings, C.J., Reinstein, E., Sun, Y., Antalffy, B., Jiang, Y., Ciechanover, A., Orr, H.T., Beaudet, A.L. and Zoghbi, H.Y. (1999) Mutation of the E6-AP ubiquitin ligase reduces nuclear inclusion frequency while accelerating polyglutamine-induced pathology in SCA1 mice. *Neuron*, **24**, 879–892.
19. Ciechanover, A. and Brundin, P. (2003) The ubiquitin proteasome system in neurodegenerative diseases. Sometimes the chicken, sometimes the egg. *Neuron*, **40**, 427–446.
20. van Leeuwen, F.W., de Kleijn, D.P., van den Hurk, H.H., Neubauer, A., Sonnemans, M.A., Sluijs, J.A., Koycu, S., Ramdjielal, R.D., Salehi, A., Martens, G.J. *et al.* (1998) Frameshift mutants of beta amyloid precursor protein and ubiquitin-B in Alzheimer's and Down patients. *Science*, **279**, 242–247.
21. Fischer, D.F., de Vos, R.A.I., van Dijk, R., de Vrij, F.M.S., Proper, E.A., Sonnemans, M.A.F., Verhage, M.C., Sluijs, J.A., Hobo, B., Zouambia, M. *et al.* (2003) Disease-specific accumulation of mutant ubiquitin as a marker for proteasomal dysfunction in the brain. *FASEB J.*, **17**, 2014–2024.
22. Lindsten, K., de Vrij, F.M., Verhoef, L.G., Fischer, D.F., van Leeuwen, F.W., Hol, E.M., Masucci, M.G. and Dantuma, N.P. (2002) Mutant ubiquitin found in neurodegenerative disorders is a ubiquitin fusion degradation substrate that blocks proteasomal degradation. *J. Cell Biol.*, **157**, 417–427.
23. De Vrij, F.M., Sluijs, J.A., Gregori, L., Fischer, D.F., Hermens, W.T., Goldgaber, D., Verhaagen, J., Van Leeuwen, F.W. and Hol, E.M. (2001) Mutant ubiquitin expressed in Alzheimer's disease causes neuronal death. *FASEB J.*, **15**, 2680–2688.
24. Lam, Y.A., Pickart, C.M., Alban, A., Landon, M., Jamieson, C., Ramage, R., Mayer, R.J. and Layfield, R. (2000) Inhibition of the ubiquitin–proteasome system in Alzheimer's disease. *Proc. Natl Acad. Sci. USA*, **97**, 9902–9906.
25. Song, S., Kim, S.Y., Hong, Y.M., Jo, D.G., Lee, J.Y., Shim, S.M., Chung, C.W., Seo, S.J., Yoo, Y.J., Koh, J.Y. *et al.* (2003) Essential role of E2-25K/Hip-2 in mediating amyloid-beta neurotoxicity. *Mol. Cell*, **12**, 553–563.
26. Keller, J.N., Hanni, K.B. and Markesbery, W.R. (2000) Impaired proteasome function in Alzheimer's disease. *J. Neurochem.*, **75**, 436–439.
27. Keck, S., Nitsch, R., Grune, T. and Ullrich, O. (2003) Proteasome inhibition by paired helical filament-tau in brains of patients with Alzheimer's disease. *J. Neurochem.*, **85**, 115–122.
28. de Cristofaro, T., Affaitati, A., Cariello, L., Avvedimento, E.V. and Varrone, S. (1999) The length of polyglutamine tract, its level of expression, the rate of degradation, and the transglutaminase activity influence the formation of intracellular aggregates. *Biochem. Biophys. Res. Commun.*, **260**, 150–158.
29. Hackam, A.S., Hodgson, J.G., Singaraja, R., Zhang, T., Gan, L., Gutekunst, C.A., Hersch, S.M. and Hayden, M.R. (1999) Evidence for both the nucleus and cytoplasm as subcellular sites of pathogenesis in Huntington's disease in cell culture and in transgenic mice expressing mutant huntingtin. *Philos. Trans R. Soc. Lond. B, Biol. Sci.*, **354**, 1047–1055.
30. Lunkes, A. and Mandel, J. (1998) A cellular model that recapitulates major pathogenic steps of Huntington's disease. *Hum. Mol. Genet.*, **7**, 1355–1361.
31. Encinas, M., Iglesias, M., Liu, Y., Wang, H., Muhaisen, A., Cena, V., Gallego, C. and Comella, J.X. (2000) Sequential treatment of SH-SY5Y cells with retinoic acid and brain-derived neurotrophic factor gives rise to fully differentiated, neurotrophic factor-dependent, human neuron-like cells. *J. Neurochem.*, **75**, 991–1003.
32. Yoshizawa, T., Yoshida, H. and Shoji, S. (2001) Differential susceptibility of cultured cell lines to aggregate formation and cell death produced by the truncated Machado–Joseph disease gene product with an expanded polyglutamine stretch. *Brain Res. Bull.*, **56**, 349–352.
33. Carrard, G., Bulteau, A.L., Petropoulos, I. and Friguet, B. (2002) Impairment of proteasome structure and function in aging. *Int. J. Biochem.Cell. Biol.*, **34**, 1461–1474.
34. Furukawa, Y., Vigouroux, S., Wong, H., Guttman, M., Rajput, A.H., Ang, L., Briand, M., Kish, S.J. and Briand, Y. (2002) Brain proteasomal function in sporadic Parkinson's disease and related disorders. *Ann. Neurol.*, **51**, 779–782.
35. Ishikawa, K., Fujigasaki, H., Saegusa, H., Ohwada, K., Fujita, T., Iwamoto, H., Komatsuzaki, Y., Toru, S., Toriyama, H., Watanabe, M. *et al.* (1999) Abundant expression and cytoplasmic aggregations of [alpha]1A voltage-dependent calcium channel protein associated with neurodegeneration in spinocerebellar ataxia type 6. *Hum. Mol. Genet.*, **8**, 1185–1193.
36. Lam, Y.A., Lawson, T.G., Velayutham, M., Zweier, J.L. and Pickart, C.M. (2002) A proteasomal ATPase subunit recognizes the polyubiquitin degradation signal. *Nature*, **416**, 763–767.
37. Michalik, A. and Van Broeckhoven, C. (2003) Pathogenesis of polyglutamine disorders: aggregation revisited. *Hum. Mol. Genet.*, **12**, 173R–186R.
38. Rubinsztein, D.C., Leggo, J., Coles, R., Almqvist, E., Biancalana, V., Cassiman, J.J., Chotai, K., Connarty, M., Crauford, D., Curtis, A. *et al.* (1996) Phenotypic characterization of individuals with 30–40 CAG repeats in the Huntington disease (HD) gene reveals HD cases with 36 repeats and apparently normal elderly individuals with 36–39 repeats. *Am. J. Hum. Genet.*, **59**, 16–22.
39. McNeil, S., Novelletto, A., Srinidhi, J., Barnes, G., Kornbluth, I., Altherr, M., Wasmuth, J., Gusella, J., MacDonald, M. and Myers, R. (1997) Reduced penetrance of the Huntington's disease mutation. *Hum. Mol. Genet.*, **6**, 775–779.
40. Li, J.L., Hayden, M.R., Almqvist, E.W., Brinkman, R.R., Durr, A., Dode, C., Morrison, P.J., Suchowersky, O., Ross, C.A., Margolis, R.L. *et al.* (2003) A genome scan for modifiers of age at onset in Huntington disease: The HD MAPS study. *Am. J. Hum. Genet.*, **73**, 682–687.
41. Trottier, Y., Lutz, Y., Stevanin, G., Imbert, G., Devys, D., Cancel, G., Saudou, F., Weber, C., David, G., Tora, L. *et al.* (1995) Polyglutamine expansion as a pathological epitope in Huntington's disease and four dominant cerebellar ataxias. *Nature*, **378**, 403–406.
42. Paulson, H.L., Das, S.S., Crino, P.B., Perez, M.K., Patel, S.C., Gotsdiner, D., Fischbeck, K.H. and Pittman, R.N. (1997) Machado–Joseph disease gene product is a cytoplasmic protein widely expressed in brain. *Ann. Neurol.*, **41**, 453–462.
43. Hol, E.M., Roelofs, R.F., Moraal, E., Sonnemans, M.A., Sluijs, J.A., Proper, E.A., de Graan, P.N., Fischer, D.F. and van Leeuwen, F.W. (2003) Neuronal expression of GFAP in patients with Alzheimer pathology and identification of novel GFAP splice forms. *Mol. Psychiat.*, **8**, 786–796.
44. Neumann, M. and Gabel, D. (2002) Simple method for reduction of autofluorescence in fluorescence microscopy. *J. Histochem. Cytochem.*, **50**, 437–439.
45. Kerstens, H.M., Poddighe, P.J. and Hanselaar, A.G. (1995) A novel *in situ* hybridization signal amplification method based on the deposition of biotinylated tyramine. *J. Histochem. Cytochem.*, **43**, 347–352.
46. Naldini, L., Blomer, U., Gallay, P., Ory, D., Mulligan, R., Gage, F.H., Verma, I.M. and Trono, D. (1996) *In vivo* gene delivery and stable transduction of nondividing cells by a lentiviral vector. *Science*, **272**, 263–267.
47. Field, J., Nikawa, J., Broek, D., MacDonald, B., Rodgers, L., Wilson, I.A., Lerner, R.A. and Wigler, M. (1988) Purification of a RAS-responsive adenylyl cyclase complex from *Saccharomyces cerevisiae* by use of an epitope addition method. *Mol. Cell. Biol.*, **8**, 2159–2165.